Polarity Control for Non-thiolated DNA Adsorption onto Gold Nanoparticles

Xu Zhang[†,‡], Biwu Liu[†], Mark R. Servos[‡] and Juewen Liu[†]*

[†]Department of Chemistry and Waterloo Institute for Nanotechnology, [‡]Department of Biology, University of Waterloo, 200 University Avenue West, Waterloo, Ontario, Canada N2L 3G1.

Email: liujw@uwaterloo.ca

Abstract

Gold nanoparticles (AuNPs) functionalized with thiolated DNA have enabled many studies in nanoscience. The strong thiol/gold affinity and the nanoscale curvature of AuNPs allow the attached DNA to adapt an upright conformation favourable for hybridization. Recently, it has been shown that non-thiolated DNA can also be attached via DNA base adsorption. Without a thiol label, both ends of the DNA and even internal bases could be adsorbed, decreasing the specificity of subsequent molecular recognition reactions. In this work, we employed a modular sequence design approach to systematically study the effect of DNA sequence on adsorption polarity. A block of poly-adenine (poly-A) could be used to achieve a high density of DNA attachment. When the poly-A block length is short (e.g. below 5-7), the loading was independent of the block length and the conjugate cannot hybridize to its cDNA effectively, suggesting a random attachment controlled by adsorption kinetics. Increasing the block length leads to reduced capacity but improved hybridization, suggesting that more DNA with the desired conformation was adsorbed due to the thermodynamic effects of poly-A binding. The design can be further improved by including capping sequences rich in T or G. Finally, a more general double-stranded DNA approach was described to be suitable for DNA that cannot satisfy the abovementioned design requirements.

Introduction

DNA-functionalized gold nanoparticles (AuNPs) have been one of the most often used reagents in nanobiotechnology since 1996,[1,2] where the physical properties of AuNPs are coupled to the structural and chemical properties of DNA. For example, the color of AuNPs is changed from red to blue upon DNA-directed assembly due to the coupling of their surface plasmon, popularizing applications in colorimetric sensing.[3-6] At the same time, many fundamental insights have been obtained using this hybrid material.[7-18] To enable these applications, the first step is DNA attachment and there are two main approaches to achieve this. This field started with thiolated DNA, where a very high DNA density can be immobilized.[1,2] This is partially due to the nanoscale curvature that allows packing of more DNA.[9] Thiolated DNA may serve as its own blocking agent to ensure that the immobilized DNAs are mainly in an upright conformation. This is in contrast to DNA-functionalized planar gold surfaces, where short-chain alkylthiols are often required to block the surface to avoid non-specific DNA base adsorption.[19] Such a dense DNA layer also helps maintain an excellent colloidal stability of the AuNPs. The conformation of DNA on AuNPs has been extensively studied using dynamic light scattering and gel electrophoresis.[17,20-22]

In 2004, non-thiolated DNA was found to protect AuNPs against salt-induced aggregation as long as the DNA is single-stranded, short and unfolded,[23,24] suggesting the adsorption of non-thiolated DNA. This adsorption process has been extensively studied and in general the DNA loading capacity is much lower than that can be achieved by thiolated DNA, suggesting a model of DNA wrapping around the AuNPs.[15,25-27] Since the interaction between DNA bases and gold is much stronger than that with the complementary DNA (cDNA), adsorbed DNA might lose its molecular recognition function. This might explain why very few reports use desorption of adsorbed non-thiolated DNA for designing biosensors. Ideally, non-thiolated DNA should adopt an upright conformation just like the thiolated counterpart to achieve molecular recognition. Very recently, this goal has been achieved in two independent reports.[28,29] Fan and co-workers used the traditional ‘salt-aging’ method to incubate DNA

containing a poly-adenine (poly-A) sequence at around neutral pH over ~3 days.[28] It was suggested that the poly-adenine fragment was adsorbed while the rest of the sequences were in the upright conformation. Alternatively, we reported that at pH 3, a short incubation of a few minutes was sufficient.[29] This is due to the protonation of DNA bases at low pH.[10] With either method, the resulting conjugate shares similar functions and properties as the thiolated counterpart, such as good colloidal stability and sharp melting transition of DNA-linked AuNP assemblies.

Studying non-thiolated DNA is important for several reasons. First, the cost of DNA synthesis can be reduced by more than 90% since it is quite expensive to add a thiol label. Second, the fundamental understanding of the interaction between DNA and gold can be further increased. Finally, new applications may be derived from this hybrid material including biosensor development,[30-37] control of enzymatic reaction,[37-39] nanoparticle synthesis,[40,41] and medicine.[40,42] The adsorption energy for a thiol label to Au is ~160 kJ/mol while the adsorption energy for a DNA nucleotide to Au is around 100-120 kJ/mol, where A and C adsorb more strongly than T.[43-46] Therefore, for a thiolated DNA, the thiol end is more likely to be adsorbed than the non-labeled end. However, for non-thiolated DNA, both the 3′ and the 5′-end and even internal bases might be adsorbed. A critical question to be answered is thus how to control the polarity of non-thiolated DNA adsorption. Since adenine is adsorbed with a higher affinity than thymine, a straightforward method is to make one end poly-A and the other end thymine rich.[28,29] Recent studies have confirmed the high stability and functionality of such non-thiolated DNA/AuNP conjugates.[28,29] While this design concept is appealing, a few further questions remain to be addressed. For example, the optimal number of adenine and its affect on DNA loading capacity need to be determined. In addition, what if the intended non-adsorbing end contains bases other than T? Finally, what if a DNA sequence has to be rich in adenine in both ends? This paper aims to address these problems by modular and rational design of DNA sequences.

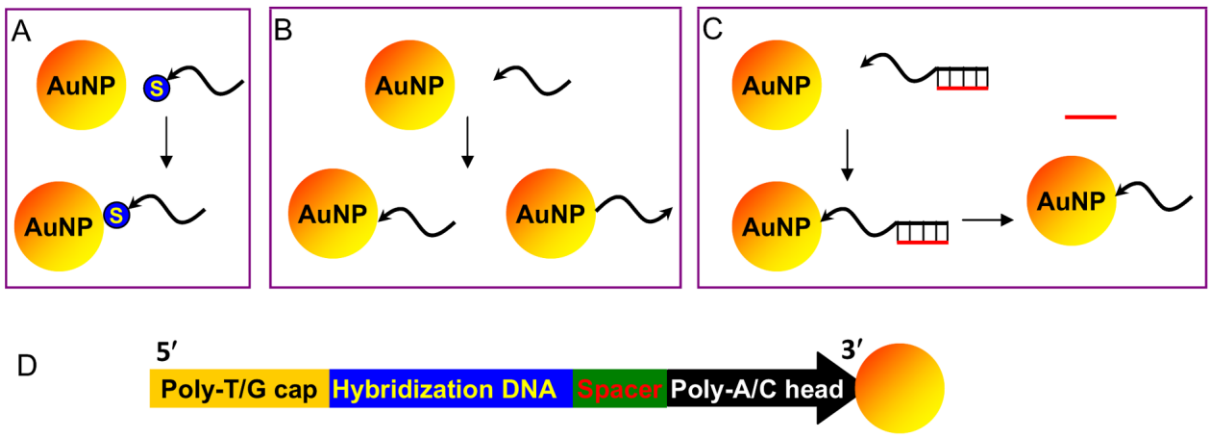

Figure 1. Schematics of DNA polarity control for adsorption onto AuNPs. (A) Adsorption of thiolated DNA takes place via the thiol group. The arrow head indicates that a DNA sequence has polarity in terms of 3′ and 5′. (B) Non-thiolated DNA could be adsorbed on either end, or even via internal bases (not shown). (C) Blocking one end of DNA by forming a partial duplex might favour the adsorption of the other end. The blocking strand could be subsequently washed away. (D) Modular design of non-thiolated DNA sequences to study DNA adsorption and polarity control.

Materials and Methods

Chemicals. All of the DNA samples were purchased from Integrated DNA Technologies (Coralville, IA) and purified by standard desalting. A partial list of DNA sequences are shown in Table 1. $HAuCl_4$ and KCN were from Sigma-Aldrich. AuNPs (13 nm) were synthesized based on the standard citrate reduction procedures with a concentration estimated to be ~10 nM.[47] Ethanol, PEG 20,000 and hydrochloric acid were purchased from VWR (Mississauga, ON). SYBR Green I was from Life Technologies Inc. Sodium citrate, sodium chloride and 4-(2-hydroxyethyl) piperazine-1-ethanesulfonate (HEPES) were purchased from Mandel Scientific (Guelph, ON). Milli-Q water was used for all experiments.

Table 1. A partial list of the DNA sequences and modifications used in this work.

DNA ID	Name	Sequences and modifications (from 5′ to 3′)
1	0A-1T	TTCACAGATGCGT
2	1A-1T	TTCACAGATGCGTA
3	3A-1T	TTCACAGATGCGTAAA
4	5A-1T	TTCACAGATGCGTAAAAA
5	7A-1T	TTCACAGATGCGTAAAAAAA
6	9A-1T	TTCACAGATGCGTAAAAAAAAA
7	12A-1T	TTCACAGATGCGTAAAAAAAAAAAA
8	15A-1T	TTCACAGATGCGTAAAAAAAAAAAAAAA
9	20A-1T	TTCACAGATGCGTAAAAAAAAAAAAAAAAAAAA
10	0C-2T	TTTCACAGATGCGT
11	1C-2T	TTTCACAGATGCGTC
12	3C-2T	TTTCACAGATGCGTCCC
13	5C-2T	TTTCACAGATGCGTCCCCC
14	7C-2T	TTTCACAGATGCGTCCCCCCC
15	9C-2T	TTTCACAGATGCGTCCCCCCCCC
16	12C-2T	TTTCACAGATGCGTCCCCCCCCCCCC
17	15C-2T	TTTCACAGATGCGTCCCCCCCCCCCCCCC
18	20C-2T	TTTCACAGATGCGTCCCCCCCCCCCCCCCCCCCC
19	9A5′	AAAAAAAAA CCCAGGTTCTCT
20	9A3T	TTTTCACAGATGCGTAAAAAAAAA
21	0A5′SH	SH-CCCAGGTTCTCT
22	Linker-3A	ACGCATCTGTGAAAA AGAGAACCTGGG
23	0A3T-3T	TTTTCACAGATGCGTTTT
24	1A3T-3T	TTTTCACAGATGCGTTTTA
25	3A3T-3T	TTTTCACAGATGCGTTTTAAA
26	5A3T-3T	TTTTCACAGATGCGTTTTAAAAA
27	7A3T-3T	TTTTCACAGATGCGTTTTAAAAAAA
28	9A3T-3T	TTTTCACAGATGCGTTTTAAAAAAAAA
29	FAM-Anti3′	ACGCATCTGTGA-FAM
30	9A-0T	TCACAGATGCGTAAAAAAAAA
31	9A-1T	TTCACAGATGCGTAAAAAAAAA
32	9A-5T	TTTTTTCACAGATGCGTAAAAAAAAA
33	9A-7T	TTTTTTTTCACAGATGCGTAAAAAAAAA
34	9A-9T	TTTTTTTTTTCACAGATGCGTAAAAAAAAA
35	9A-0G	TCACAGATGCGTAAAAAAAAA
36	9A-1G	GTCACAGATGCGTAAAAAAAAA
37	9A-2G	GGTCACAGATGCGTAAAAAAAAA
38	9A-4G	GGGGTCACAGATGCGTAAAAAAAAA
39	9A-5G	GGGGGTCACAGATGCGTAAAAAAAAA
40	9A3′	TCACAGATGCGTAAAAAAAAA
41	9A3′a	TTCTGTATGCGTAAAAAAAAA
42	9A3′b	TTGTCGTTGCGTAAAAAAAAA
43	9A3′c	TTGTGTGTGCGTAAAAAAAAA
44	9A3′SH	TCACAGATGCGTAAAAAAAAA-SH

45	Linker	ACGCATCTGTGAAGAGAACCTGGG
46	Linker-a	ACGCATACAGAAAGAGAACCTGGG
47	Linker-b	ACGCAACGACAAAGAGAACCTGGG
48	Linker-c	ACGCACACACAAAGAGAACCTGGG
49	9A5′SH	SH-AAAAAAAAACCCAGGTTCTCT

Functionalization of AuNPs with single-stranded (ss)-DNA. To prepare DNA-AuNP conjugates, regardless of DNA sequence or modification, the general procedure includes four steps. First, a small volume (i.e., 1-3 μL) of DNA stock solution (100 μM in 5 mM HEPES buffer, pH 7.6) was added into 200 μL of as-synthesized 13 nm AuNP solution (10 nM) and mixed by a brief vortex. Second, pH 3 citrate buffer was added into the AuNP solution to make a final citrate concentration of 10 mM. After 3 min incubation at room temperature, the pH of the AuNP solution was adjusted back to neutral by adding 500 mM HEPES buffer to a final HEPES concentration of 30 mM (pH 7.6). The sample was incubated for another 5-10 min. Finally, the DNA-AuNP mixture was centrifuged at 15,000 rpm and the supernatant was removed. The pellet was washed with 5 mM HEPES to remove free DNA. This centrifugation and washing procedure was repeated 4-5 times to ensure complete removal of free DNA and the conjugate was dispersed in 5 mM HEPES buffer for further use.

Quantification of the adsorbed DNA. The adsorbed DNA was released from AuNPs by dissolving the AuNPs with a small volume of 1 M KCN solution (final [KCN] = 20 mM). For FAM-labeled DNA, the quantification was performed by determining the fluorescence intensity of the diluted KCN-treated sample with a plate reader (Infinite F200 Pro, Tecan). A calibration curve was built by plotting the fluorescence intensity of each standard over the concentration series. For non-labeled DNAs, SYBR Green I with a final concentration of 2 μM in each well was employed for KCN treated samples. The calibration curve was built with a series of DNA concentration standards (e.g. 0, 5, 10, 20, 50 nM DNA, n = 3). The background signal was obtained from the wells containing the dye but without DNA, and the background was subtracted.

Long-term DNA adsorption kinetics. To compare the adsorption kinetics of DNA19 using the pH 3 method with the salt aging method at pH 7, DNA density on AuNPs was measured as a function of time. For salt aging, first, DNA stock in 5 mM HEPES buffer (100 μM) was added into 500 μL of AuNP solutions (10 nM) to reach a ratio of 200 DNA/AuNP and incubated for 16 hours (n = 2). Afterwards, NaCl was added (final concentration = 100 mM) to enhance DNA adsorption. The pH 3 method was the same as described above. The time points for sampling were 1, 1.5, 16, 17, 24, 48, and 80 hr. At each time points, 50 μL of DNA-AuNP solution was collected from each sample and the free DNAs were removed by three centrifugation and re-dispersion cycles before using KCN to dissolve AuNPs for SYBR Green-based quantification.

DNA-directed assembly. First, non-thiolated DNA-functionalized AuNPs were respectively mixed with AuNPs functionalized with DNA49. Assembly took place in 150 mM NaCl with 250 nM linker DNA. For comparison, a control sample was prepared containing the same amount of DNA-AuNPs and NaCl, but with a 24-mer DNA non-complementary DNA. The mixture in the sample tube changed color to purple after only 10 min incubation at room temperature, indicating the formation of AuNP aggregates; the aggregates precipitated after 2 hrs at 4 °C. The samples were characterized by a UV-vis spectrometer (Agilent 8453A) and also recorded by a digital camera (PowerShot SD 1000, Canon).

Functionalization of AuNPs using the double-stranded (ds)-DNA method. The ds-DNA was prepared by mixing DNA40 with DNA29 at a ratio of 1:1 (50 μM each) in the presence of 200 mM NaCl. To facilitate duplex formation, the mixture was heated to 90 °C for 2 min, cooled to room temperature in 30 min and then incubated at 4 °C for 2 hrs. Prior to adding the ds-DNA into AuNPs in a molar ratio of 100:1, the AuNPs were dispersed in 2.5% PEG 20,000 and then 180 mM NaCl was added. The DNA-AuNP mixture was incubated overnight at room temperature for DNA attachment. The free DNAs were removed by rinsing with HEPES buffer (5 mM) and then with Milli-Q water via centrifugation. The cDNA was dissociated by 2 hr incubation in the presence of 60 mM NaOH (pH 11).

Afterwards, the functionalized AuNPs were rinsed twice and re-dispersed in 5 mM HEPES for use. For measuring the hybridization efficiency (defined by the ratio of number of hybridized DNA29 to that of the immobilized DNA40), DNA40-functionalized AuNP was hybridized with DNA29 in the ratio of 1:50 in 200 mM NaCl over 24 hrs at room temperature. The free DNA29 was removed by centrifugation at 15,000 rpm in 4 °C. De-hybridization was performed by 2 hr incubation in 60 mM NaOH. The supernatant after centrifugation was collected and neutralized with 500 mM HEPES buffer (pH 7.6) before measuring fluorescence with the plate reader.

Results and Discussion

Intrinsic polarity preference of non-thiolated DNA adsorption. For thiolated DNA, it is generally accepted that DNA adsorption occurs via the thiol (Figure 1A). For non-thiolated DNA, an interesting question is whether there is an intrinsic preference for a DNA to be adsorbed via the 3′ or 5′-end. From the structural standpoint, DNA bases are not shielded on either end and there is unlikely to be a difference. To test this, we measured the adsorption capacity of a number of 15-mer DNAs using the low pH DNA loading method. Compared to DNA loading at neutral pH taking a few days,[28] a few minutes are sufficient to attach DNA to AuNPs at pH 3.[10,29] Two sets of DNA sequences were designed with the middle 13 nucleotides being A_{13} or C_{13}, respectively. For each set of DNA, the two ends were A or T, yielding a total of four sequences in each set. The adsorbed DNA was quantified using SYBR Green I as a staining dye. We found that significantly more DNA was adsorbed when both ends were A than T (Figure 2). However, there was little difference when A and T were both present, regardless of whether A is on the 3′ or 5′ end. This experiment confirms the lack of intrinsic preference for either end of DNA, and polarity control might be realized by adjusting the DNA sequence. One way to achieve adsorption polarity control is to intentionally place a poly-A block to serve as an anchor on AuNPs (e.g. a replacement of the thiol functionality) and T on the other end to encourage an upright conformation.

Because of its high affinity, the poly-A anchor might displace DNA adsorption via the T end.[28] Next we studied the length of the poly-A block.

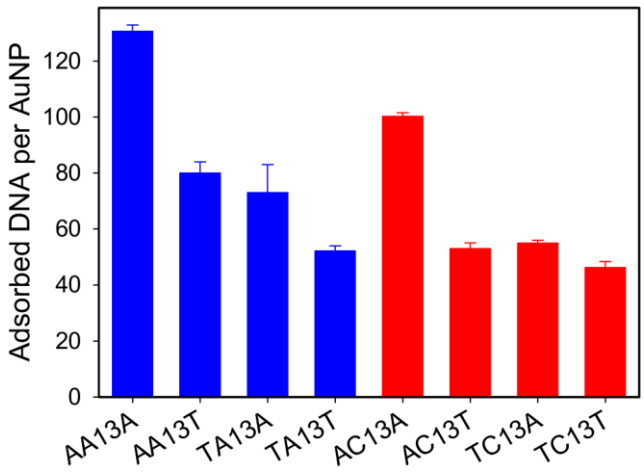

Figure 2. Adsorption capacity of non-thiolated 15-mer DNA by AuNPs using the low pH DNA loading method. The DNA sequences are listed in the *x*-axis (start from the 5′-end). Note that these sequences are not included in Table 1. Note that 100 DNA per AuNP (13 nm diameter) equals to 18.8×10^{12} DNA/cm^2 of gold surface.

Effect of poly-A length. To systematically optimize DNA sequence we employed a modular design (Figure 1D). The head sequence is poly-A or poly-C since they have a high affinity towards gold surfaces. Following the poly-A/C block, there is an optional poly-T space, which may discourage the next module (i.e. sequence for hybridization) from interacting with the gold surface. We chose to use a 12-nucleotide hybridization sequence since this is a commonly used probe length. Finally, the tail module may contain a few thymines or guanines as a cap to favour adsorption from the poly-A end.

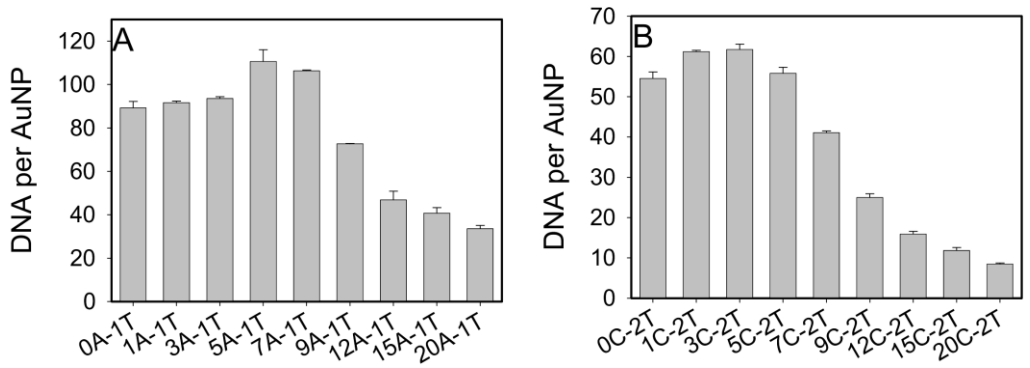

Figure 3. DNA adsorption capacity as a function of the length of poly-A (A) or poly-C (B). DNA1 to 9 were used for (A) and DNA10 to 18 for (B). Note that 100 DNA per AuNP (13 nm diameter) equals to 18.8×10^{12} DNA/cm^2 of gold surface.

We first varied the number of adenine bases in the tail from 0 to 20 (Table 1, DNA ID=1-9). As shown in Figure 3A, a similar loading of ~90 DNA per AuNP was observed from 0A to 7A. Fan and co-workers reported that the loading of poly-A DNA at neutral pH was a function of DNA length, and longer DNA has a lower capacity but the overall adenine number remained roughly the same (e.g. ~400 adenine per 13 nm AuNP), suggesting that every adenine nucleotide in the poly-A block was adsorbed onto the AuNP.[28] In our low pH case, however, from 0 to 7 adenines, the number of adenine has little effect on the loading capacity, suggesting that only the terminal one or a few bases are responsible for DNA adsorption. With even longer adenine spacer, the adsorption capacity clearly showed an adenine length-dependent decrease as reported by Fan. Therefore, our result indicates two interaction regions corresponding to the poly-A length. When the adenine number is below 7, it appears that end adsorption via one or a few bases is a good description, but beyond that full adenine adsorption might be more appropriate. From the thermodynamic perspective, it is more likely that adsorption takes place through all the adenines in the poly-A block to take the multivalent advantage. But at low pH, the kinetics is so fast that it may dominate the adsorption process when the poly-A block is short.

Many previous assays indicated that in addition to adenine, cytosine can also be tightly adsorbed by gold.[43-46] Thus, poly-C might also serve as an anchoring block. Herein we measured the DNA loading capacity as a function of the length of poly-C (Figure 3B). A similar trend was observed, where the DNA loading was quite independent of the number of cytosine when the block length was shorter than five while decreased loading was observed with longer cytosine blocks.

Comparison of pH effect. Since non-thiolated DNA can be adsorbed either at pH 3 for a few minutes or at neutral pH with NaCl for a few days. A systematic comparison of these two methods might provide important mechanistic insights. Towards this goal, we followed the loading of DNA19 with a 9-adenine block as a function of time. When the DNA was loaded at pH 3, the initial capacity was high (~90 per AuNP, Figure 4A). After the first a few minutes to load the DNA, the pH was adjusted to 7. The adsorbed DNA was quantified at designated time points for more than 3 days. In the initial a few hours the loading was quite stable, but after ~20 hrs the loading was decreased to ~50 DNA per AuNPs. The loading remained as such for the next 2 to 3 days, suggesting that a thermodynamically stable state was reached. On the other hand, using the salt aging method at pH 7, the initial capacity was very low. A final concentration of 100 mM NaCl was added at 16 hr, when a significant increase in the loading was observed. Saturated adsorption was achieved in ~ 2 days. After that, the capacity of these two conditions converged, suggesting both reached a similar equilibrium state. The schemes of DNA adsorption under these two conditions are shown in Figure 4B.

Combined with the above poly-A length-dependent adsorption capacity, we reason that when the poly-A block is short (e.g. below 7 adenines), the multivalent effect is not pronounced under the fast adsorption kinetics condition at pH 3 and the DNA might be adsorbed via a wide range of conformations. When the poly-A block is long (e.g. more than 7 adenines), they can quickly be adsorbed via the A block and displace the other low affinity nucleotides, resulting in a much lower adsorption capacity. It needs to be noted that the critical poly-A length is based on the 12-mer

hybridization sequence; it is likely that the critical poly-A length will increase for longer hybridization sequences.

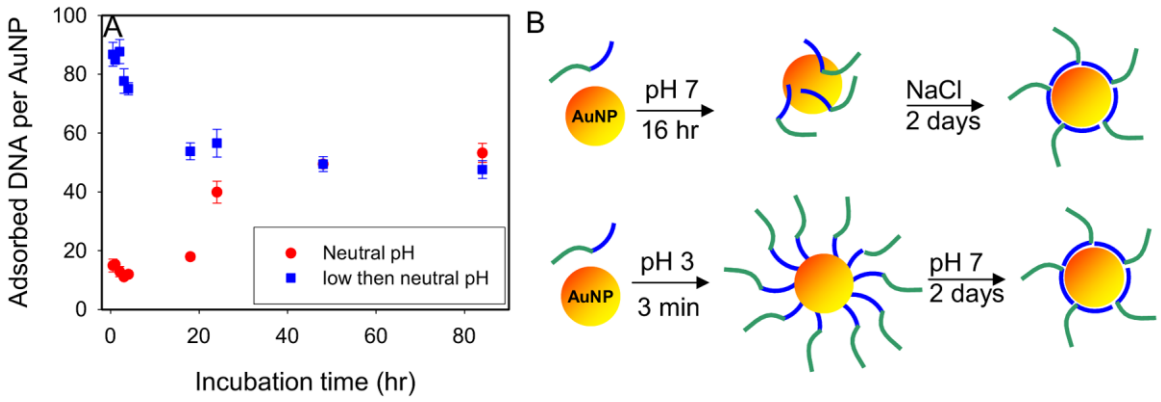

Figure 4. (A) Change of DNA loading capacity as a function of incubation time at pH 3 and pH 7. Note that the pH 3 sample was incubated at pH 3 for only 3 min before it was adjusted back to neutral pH. For the pH 7 sample, 100 mM NaCl was added at 16 hr. (B) Schematics of non-thiolated DNA adsorption by salt aging at neutral pH or by the low pH method. The blue block represents poly-A and the green part is intended to be in an upright conformation for further hybridization reactions.

DNA-directed assembly. DNA adsorption polarity is particularly important for DNA-directed assembly. When AuNPs are assembled by linker DNA, there is a shift in the surface plasmon band that can be monitored using UV-vis spectroscopy. Unmodified AuNPs have a sharp peak at 520 nm (Figure 5A, black spectrum). In the absence of linker DNA, AuNPs functionalized with non-thiolated DNA20 with a 9-adenine block have a similar shape, suggesting that the AuNPs were quite stable even after incubating in 150 mM NaCl overnight. With linker (DNA22, Table 1) and AuNPs functionalized with DNA21, the 520 nm peak decreased intensity while the 650 nm region increased. Therefore, the ratio of extinction at 520 nm over 650 nm was used to quantify the aggregation state. Dispersed AuNPs have

a high ratio of ~12 while aggregated AuNPs are much lower. We compared all the samples with different non-thiolated DNA (DNA23-28) with and without linker DNA (Figure 5B). As long as the DNA contained more than 3 adenines, the stability of the AuNPs was very good since the samples without the linker DNA showed a high ratio. If the poly-A block was too short, the AuNPs aggregated even without linker DNA. With the linker DNA, all the samples showed a decrease in the extinction ratio, indicating formation of aggregated AuNPs. This experiment indicates the minimal poly-A block length to be 3 to 5 to achieve good DNA-directed assembly.

Next we measured the rate of hybridization using FAM-labeled cDNA (DNA29) so that the reaction kinetics can be followed using fluorescence quenching (Figure 5C). Compared to the DNA-directed assembly assays, this fluorescence assay is more stringent. For example, a few DNAs with the upright conformation can achieve the assembly, but to obtain a large fluorescence decrease, most DNA needs to be in the upright conformation. Interestingly, there is also a strong correlation between the poly-A length and hybridization kinetics. In general, a longer poly-A block gives faster hybridization. When the adenine block is shorter than 5, the hybridization kinetics are very slow. This trend agrees with the AuNP aggregation assay in Figure 5B. When the poly-A length is greater than 12, no further increase of hybridization rate is observed. It is likely that a longer poly-A spacer produces more sparsely distributed DNA to facilitate hybridization. When the DNAs are sufficiently sparse, no further gain can be achieved. When the poly-A block is shorter than 5, a large fraction the DNA might be adsorbed via a non-optimal conformation despite the high capacity of such adsorbed DNA. The optimal adsorption conformation is achieved with more than 7 adenines, which also agrees with the capacity data in Figure 3A. In contrast to poly-A serving as an effective anchor on AuNP surfaces, it is intriguing to note that DNAs containing poly-C blocks are not functional for hybridization when they are immobilized on AuNPs (Figure 5D). They cannot perform DNA-directed assembly either (data not shown). The reason behind this observation is unclear at this point.

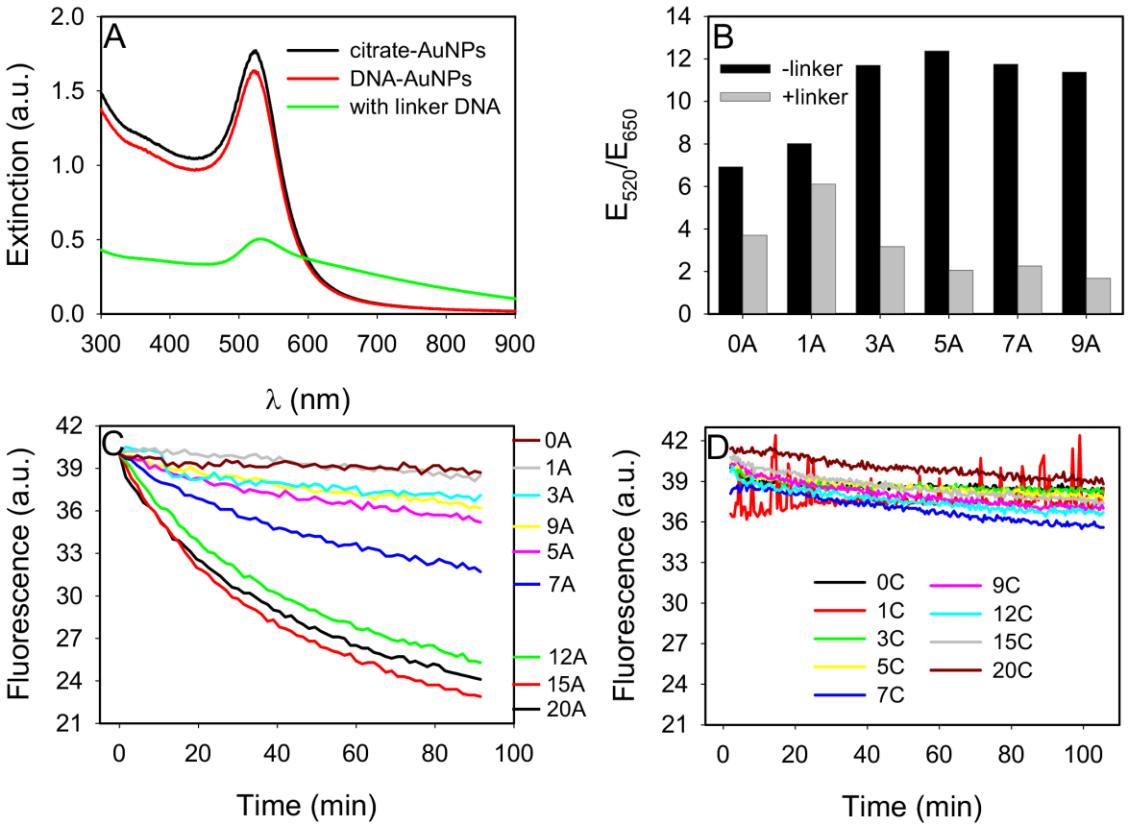

Figure 5. (A) UV-vis extinction spectra of free citrate-capped AuNPs, AuNPs functionalized with DNA20 in 150 mM NaCl, and after assembly with DNA21-functionalized AuNPs with linker (DNA22). (B) Extinction ratio indicative of the assembly state of AuNPs with or without linker DNA. The *x*-axis includes AuNPs functionalized with DNA23-28. Hybridization kinetics probed using a FAM-labeled DNA (DNA29) with AuNPs functionalized with DNA1-9 (C) and with DNA10-18 (D).

The cap sequences. To encourage the hybridization sequence to take an upright conformation, it is logical to place a few nucleotides with low affinity to gold surface such as thymine as a cap. However, there is a possibility that a poly-T cap might interact with the poly-A anchor to form a stem-loop structure, complicating adsorption and subsequent hybridization reactions. The hypothesis was verified by investigating the loading capacity of DNAs with a 9-adenine anchor and various numbers of thymine from 0 to 9 as the cap (DNA30-34, Figure 6A). The loading decreased with increasing number

of thymine, consistent with hairpin formation. The hybridization kinetics (Figure 6C) with the cDNA shows that 3 thymines are optimal. To minimize poly-T cap reacting with the poly-A block, we further evaluated poly-G caps. Figure 6B shows the change of DNA loading capacity as a function of poly-G length, where a longer poly-G cap reduces the loading capacity significantly. Meanwhile, the hybridization kinetics increase with more guanines. It is likely that more DNA was adsorbed via the poly-A end and there was little non-specific poly-G and poly-A interactions, favoring DNA into the upright conformation.

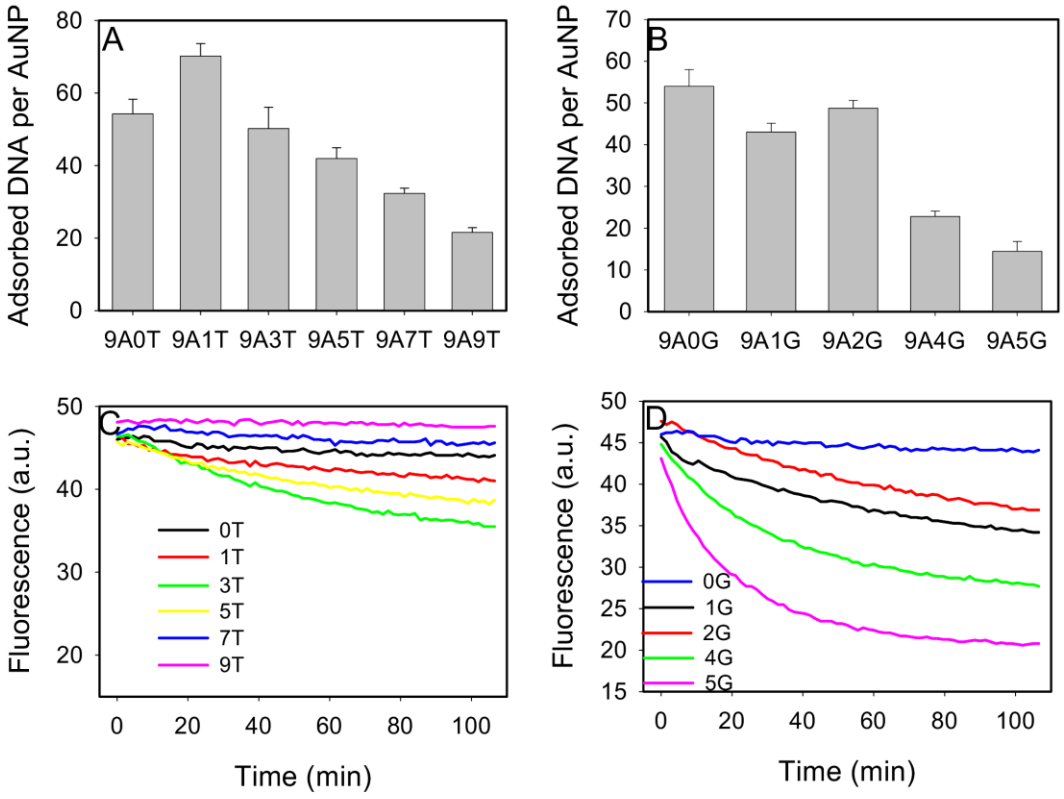

Figure 6. DNA loading capacity as a function of the length of the poly-T cap (DNA30-34) (A) or poly-G cap (DNA35-39) (B). DNA hybridization kinetics probed by a FAM-labeled DNA as a function of the length of the poly-T cap (C) or poly-G cap (D).

Capping with ds-DNA. While the above modular design might work for most applications, it is quite easy to conceive exceptions. For example, it might be necessary to attach DNA sequences that cannot be capped by T or G rich ends. In one case, we found that adding a 9A block to one of the 12-mer hybridization sequences (DNA40, see Figure 7A) cannot generate functional AuNP conjugates. There was no color change when linker DNA was added for DNA-directed assembly (Figure 7B) and fluorescence also failed to drop when a complementary FAM-labeled DNA was added (Figure 7D, green line). The DNA loading capacity remains quite high for this sample, where more than 50 DNA per AuNP were attached (Figure 7E, the last bar). A careful examination of the DNA sequence revealed that quite a few A and C are on the other end, despite the fact that the terminal base is a T (Figure 7A). One way to solve this is to change the capping sequence to introduce more T and G (e.g. using DNA41-43), where DNA-directed assembly was indeed observed for all the sequences (Figure 7C).

If, however, the terminal sequences cannot be changed, other strategies need to be derived to control adsorption polarity. One way to achieve this is to block the end intended for hybridization with a cDNA to generate a poly-A overhang, upon which AuNPs will be attached (Figure 1C). In other words, the ds-DNA part serves as a non-adsorbing cap and this is likely to be a general method. To test this, we first hybridized DNA40 with DNA29 to form a 12-mer ds-DNA with a 9-adenine overhang. Due to blocking of the DNA bases by the cDNA, adsorption could only take place via the poly-A block. In the experiment, the AuNPs were pre-treated with 2.5% polyethylene glycol (PEG, molecular weight = 20,000) and then 150 mM NaCl. PEG was used to stabilize AuNPs against salt-induced aggregation while NaCl was used to stabilize the DNA duplex and to screen the charge repulsion between DNA and AuNPs for DNA attachment.[48] We did not use the low pH method since ds-DNA denatures at such low pH. After the conjugation, the cDNA was removed at pH 11.

The loading capacity of the probe DNA was measured (Figure 7E) and their hybridization efficiency to the cDNA was compared. The loading capacity using the ds-DNA method (40 ± 3 DNA/AuNP) is lower than that of using DNA40 alone (54 ± 4) or using the thiolated version DNA44

(76 ± 5), attributable to the bulkiness of the ds-DNA compared to ss-DNA. Despite a lower loading capacity, the hybridization efficiency of AuNPs prepared using the ds-DNA approach (48% ± 6%) was much higher than that using the ss-DNA approach, approaching the efficiency of using the thiolated DNA (62% ± 5%, Figure 7D). Therefore, the ds-DNA approach is effective for controlling the polarity of DNA adsorption.

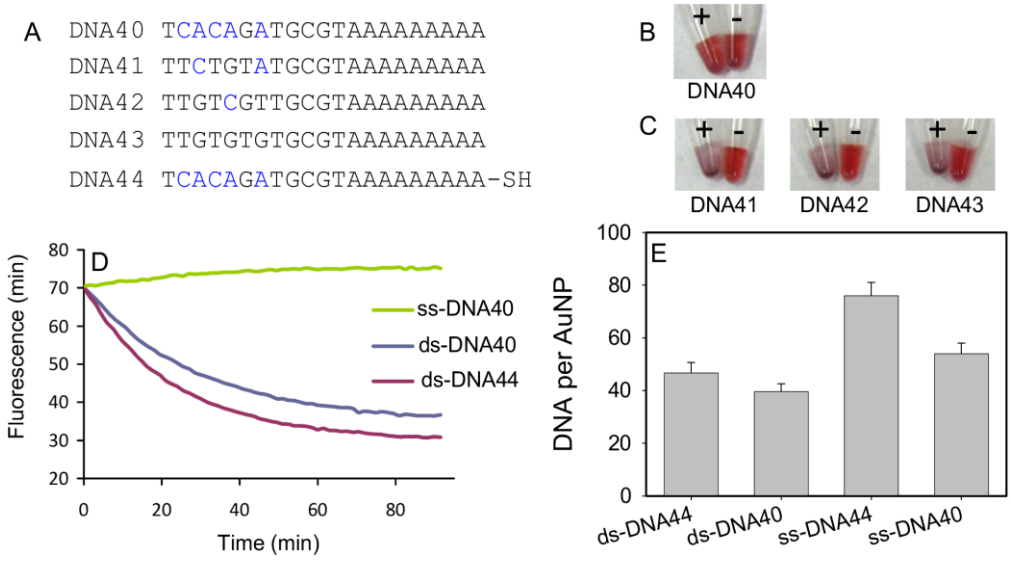

Figure 7. (A) DNA sequences used in this figure. A and C on the 5′ portion are highlighted in blue. Photographs of DNA-directed assembly using DNA40 (B), or using DNA41-43 (C). The tubes on the left contain the linker DNAs. (D) Kinetics of fluorescence decrease indicating hybridization between DNA29 and AuNPs functionalized in different ways. (E) DNA loading capacity using either the direct ss-DNA method or by forming ds-DNA first and then washing away the cDNA.

Conclusions.

In summary, we have systematically studied the effect of DNA sequence for non-thiolated DNA adsorption by AuNPs. There is no intrinsic preference for a DNA to be adsorbed on the 3′ or 5′-end, and such preference can be introduced by engineering DNA sequences. When a DNA with 12-mer hybridization sequence is terminated by a block of poly-A and if the poly-A length is longer than 5-7, the thermodynamic effect of poly-A being stronger binders takes effect, where the DNA is likely to be adsorbed via this block. If the poly-A block is too short (e.g. shorter than 3), DNA is likely to be adsorbed via many different conformations and the kinetic effect dominates. While poly-C can also bind AuNPs strongly with a similar length-dependent adsorption capacity, such DNA functionalized AuNPs cannot be used to hybridize with the cDNA. The capping sequence can be a few T or G, where G seems to offer better hybridization kinetics. In addition to this modular design based on ss-DNA, a complementary strategy is to block part of the DNA intended for hybridization by forming a duplex so that the block intended for attaching to AuNPs can be exposed to improve adsorption polarity control.

Acknowledgments

Funding for this work is from the University of Waterloo, Canadian Institutes of Health Research (CIHR), the Canadian Foundation for Innovation, and the Natural Sciences and Engineering Research Council (NSERC) of Canada and the Early Researcher Award from the Ontario Ministry of Research and Innovation.

References

(1) Mirkin, C. A.; Letsinger, R. L.; Mucic, R. C.; Storhoff, J. J. A DNA-Based Method for Rationally Assembling Nanoparticles into Macroscopic Materials. *Nature* **1996,** *382*, 607-609.

(2) Alivisatos, A. P.; Johnsson, K. P.; Peng, X.; Wilson, T. E.; Loweth, C. J.; Bruchez, M. P., Jr; Schultz, P. G. Organization of 'Nanocrystal Molecules' Using DNA. *Nature* **1996,** *382*, 609-611.

(3) Rosi, N. L.; Mirkin, C. A. Nanostructures in Biodiagnostics. *Chem. Rev.* **2005,** *105*, 1547-1562.

(4) Zhao, W.; Brook, M. A.; Li, Y. Design of Gold Nanoparticle-Based Colorimetric Biosensing Assays. *ChemBioChem* **2008,** *9*, 2363-2371.

(5) Wang, H.; Yang, R. H.; Yang, L.; Tan, W. H. Nucleic Acid Conjugated Nanomaterials for Enhanced Molecular Recognition. *ACS Nano* **2009,** *3*, 2451-2460.

(6) Liu, J.; Cao, Z.; Lu, Y. Functional Nucleic Acid Sensors. *Chem. Rev.* **2009,** *109*, 1948–1998.

(7) Lee, O. S.; Prytkova, T. R.; Schatz, G. C. Using DNA to Link Gold Nanoparticles, Polymers, and Molecules: A Theoretical Perspective. *J. Phys. Chem. Lett.* **2010,** *1*, 1781-1788.

(8) Jin, R.; Wu, G.; Li, Z.; Mirkin, C. A.; Schatz, G. C. What Controls the Melting Properties of DNA-Linked Gold Nanoparticle Assemblies? *J. Am. Chem. Soc.* **2003,** *125*, 1643-1654.

(9) Hill, H. D.; Millstone, J. E.; Banholzer, M. J.; Mirkin, C. A. The Role Radius of Curvature Plays in Thiolated Oligonucleotide Loading on Gold Nanoparticles. *ACS Nano* **2009,** *3*, 418-424.

(10) Zhang, X.; Servos, M. R.; Liu, J. Instantaneous and Quantitative Functionalization of Gold Nanoparticles with Thiolated DNA Using a pH-Assisted and Surfactant-Free Route. *J. Am. Chem. Soc.* **2012,** *134*, 7266–7269.

(11) Harris, N. C.; Kiang, C. H. Disorder in DNA-Linked Gold Nanoparticle Assemblies. *Phys. Rev. Lett.* **2005,** *95*, 046101.

(12) Maye, M. M.; Nykypanchuk, D.; van der Lelie, D.; Gang, O. A Simple Method for Kinetic Control of DNA-Induced Nanoparticle Assembly. *J. Am. Chem. Soc.* **2006,** *128*, 14020-14021.

(13) Smith, B. D.; Dave, N.; Huang, P.-J. J.; Liu, J. Assembly of DNA-Functionalized Gold Nanoparticles with Gaps and Overhangs in Linker DNA. *J. Phys. Chem. C* **2011,** *115*, 7851-7857.

(14) Sikder, M. D. H.; Gibbs-Davis, J. M. The Influence of Gap Length on Cooperativity and Rate of Association in DNA-Modified Gold Nanoparticle Aggregates. *J. Phys. Chem. C* **2012,** *116*, 11694-11701.

(15) Sandstrom, P.; Akerman, B. Electrophoretic Properties of DNA-Modified Colloidal Gold Nanoparticles. *Langmuir* **2004,** *20*, 4182-4186.

(16) Brown, K. A.; Park, S.; Hamad-Schifferli, K. Nucleotide-Surface Interactions in DNA-Modified Au-Nanoparticle Conjugates: Sequence Effects on Reactivity and Hybridization. *J. Phys. Chem. C* **2008,** *112*, 7517-7521.

(17) Park, S.; Brown, K. A.; Hamad-Schifferli, K. Changes in Oligonucleotide Conformation on Nanoparticle Surfaces by Modification with Mercaptohexanol. *Nano Lett.* **2004,** *4*, 1925-1929.

(18) Liu, J. Adsorption of DNA onto Gold Nanoparticles and Graphene Oxide: Surface Science and Applications. *Phys. Chem. Chem. Phys.* **2012,** *14*, 10485-10496.

(19) Herne, T. M.; Tarlov, M. J. Characterization of DNA Probes Immobilized on Gold Surfaces. *J. Am. Chem. Soc.* **1997,** *119*, 8916-8920.

(20) Pellegrino, T.; Sperling, R. A.; Alivisatos, A. P.; Parak, W. J. Gel Electrophoresis of Gold-DNA Nanoconjugates. *J. Biomed. Biotechnol.* **2007,** *2007*, 26796.

(21) Park, S.; Hamad-Schifferli, K. Evaluation of Hydrodynamic Size and Zeta-Potential of Surface-Modified Au Nanoparticle-DNA Conjugates via Ferguson Analysis. *J. Phys. Chem. C* **2008,** *112*, 7611-7616.

(22) Xu, J.; Craig, S. L. Thermodynamics of DNA Hybridization on Gold Nanoparticles. *J. Am. Chem. Soc.* **2005,** *127*, 13227-13231.

(23) Li, H.; Rothberg, L. J. Label-Free Colorimetric Detection of Specific Sequences in Genomic DNA Amplified by the Polymerase Chain Reaction. *J. Am. Chem. Soc.* **2004,** *126*, 10958-10961.

(24) Li, H.; Rothberg, L. Colorimetric Detection of DNA Sequences Based on Electrostatic Interactions with Unmodified Gold Nanoparticles. *Proc. Natl. Acad. Sci. U.S.A.* **2004,** *101*, 14036-14039.

(25) Nelson, E. M.; Rothberg, L. J. Kinetics and Mechanism of Single-Stranded DNA Adsorption onto Citrate-Stabilized Gold Nanoparticles in Colloidal Solution. *Langmuir* **2011,** *27*, 1770-1777.

(26) Zhang, X.; Servos, M. R.; Liu, J. Surface Science of DNA Adsorption onto Citrate-Capped Gold Nanoparticles. *Langmuir* **2012,** *28*, 3896-3902.

(27) Sandstrom, P.; Boncheva, M.; Akerman, B. Nonspecific and Thiol-Specific Binding of DNA to Gold Nanoparticles. *Langmuir* **2003,** *19*, 7537-7543.

(28) Pei, H.; Li, F.; Wan, Y.; Wei, M.; Liu, H.; Su, Y.; Chen, N.; Huang, Q.; Fan, C. Designed Diblock Oligonucleotide for the Synthesis of Spatially Isolated and Highly Hybridizable Functionalization of DNA-Gold Nanoparticle Nanoconjugates. *J. Am. Chem. Soc.* **2012,** *134*, 11876-11879.

(29) Zhang, X.; Liu, B.; Dave, N.; Servos, M. R.; Liu, J. Instantaneous Attachment of an Ultrahigh Density of Nonthiolated DNA to Gold Nanoparticles and Its Applications. *Langmuir* **2012,** *28*, 17053-17060.

(30) Li, H.; Liang, R.; Turner, D. H.; Rothberg, L. J.; Duan, S. Selective Quenching of Fluorescence from Unbound Oligonucleotides by Gold Nanoparticles as a Probe of RNA Structure. *RNA* **2007,** *13*, 2034-2041.

(31) Zhang, J.; Wang, L. H.; Pan, D.; Song, S. P.; Boey, F. Y. C.; Zhang, H.; Fan, C. H. Visual Cocaine Detection with Gold Nanoparticles and Rationally Engineered Aptamer Structures. *Small* **2008,** *4*, 1196-1200.

(32) Wang, Z.; Lee, J. H.; Lu, Y. Label-Free Colorimetric Detection of Lead Ions with a Nanomolar Detection Limit and Tunable Dynamic Range by Using Gold Nanoparticles and DNAzyme. *Adv. Mater.* **2008,** *20*, 3263-3267.

(33) Wang, W. J.; Chen, C. L.; Qian, M. X.; Zhao, X. S. Aptamer Biosensor for Protein Detection Using Gold Nanoparticles. *Anal. Biochem.* **2008,** *373*, 213-219.

(34) Wei, H.; Li, B.; Li, J.; Dong, S.; Wang, E. Dnazyme-Based Colorimetric Sensing of Lead (Pb^{2+}) Using Unmodified Gold Nanoparticle Probes. *Nanotechnology* **2008,** *19*, 095501.

(35) Wang, L.; Liu, X.; Hu, X.; Song, S.; Fan, C. Unmodified Gold Nanoparticles as a Colorimetric Probe for Potassium DNA Aptamers. *Chem. Comm.* **2006**, 3780-3782.

(36) Wang, J.; Wang, L. H.; Liu, X. F.; Liang, Z. Q.; Song, S. P.; Li, W. X.; Li, G. X.; Fan, C. H. A Gold Nanoparticle-Based Aptamer Target Binding Readout for Atp Assay. *Adv. Mater.* **2007,** *19*, 3943-3946.

(37) Zheng, X.; Liu, Q.; Jing, C.; Li, Y.; Li, D.; Luo, W.; Wen, Y.; He, Y.; Huang, Q.; Long, Y.-T.; Fan, C. Catalytic Gold Nanoparticles for Nanoplasmonic Detection of DNA Hybridization. *Angew. Chem., Int. Ed.* **2011,** *50*, 11994-11998.

(38) Li, H. K.; Huang, J. H.; Lv, J. H.; An, H. J.; Zhang, X. D.; Zhang, Z. Z.; Fan, C. H.; Hu, J. Nanoparticle Pcr: Nanogold-Assisted Pcr with Enhanced Specificity. *Angew. Chem. Int. Ed.* **2005,** *44*, 5100-5103.

(39) Park, K. S.; Kim, M. I.; Cho, D.-Y.; Park, H. G. Label-Free Colorimetric Detection of Nucleic Acids Based on Target-Induced Shielding against the Peroxidase-Mimicking Activity of Magnetic Nanoparticles. *Small* **2011,** *7*, 1521-1525.

(40) Wang, Z.; Zhang, J.; Ekman, J. M.; Kenis, P. J. A.; Lu, Y. DNA-Mediated Control of Metal Nanoparticle Shape: One-Pot Synthesis and Cellular Uptake of Highly Stable and Functional Gold Nanoflowers. *Nano Lett.* **2010,** *10*, 1886-1891.

(41) Xu, L.; Zhu, Y.; Ma, W.; Chen, W.; Liu, L.; Kuang, H.; Wang, L.; Xu, C. New Synthesis Strategy for DNA Functional Gold Nanoparticles. *J. Phys. Chem. C* **2011,** *115*, 3243-3249.

(42) Rosi, N. L.; Giljohann, D. A.; Thaxton, C. S.; Lytton-Jean, A. K. R.; Han, M. S.; Mirkin, C. A. Oligonucleotide-Modified Gold Nanoparticles for Intracellular Gene Regulation. *Science* **2006,** *312*, 1027-1030.

(43) Demers, L. M.; Oestblom, M.; Zhang, H.; Jang, N.-H.; Liedberg, B.; Mirkin, C. A. Thermal Desorption Behavior and Binding Properties of DNA Bases and Nucleosides on Gold. *J. Am. Chem. Soc.* **2002,** *124*, 11248-11249.

(44) Ostblom, M.; Liedberg, B.; Demers, L. M.; Mirkin, C. A. On the Structure and Desorption Dynamics of DNA Bases Adsorbed on Gold: A Temperature-Programmed Study. *J. Phys. Chem. B* **2005,** *109*, 15150-15160.

(45) Boland, T.; Ratner, B. D. Direct Measurement of Hydrogen Bonding in DNA Nucleotide Bases by Atomic Force Microscopy. *Proc. Natl. Acad. Sci. U.S.A.* **1995,** *92*, 5297-5301.

(46) Gourishankar, A.; Shukla, S.; Ganesh, K. N.; Sastry, M. Isothermal Titration Calorimetry Studies on the Binding of DNA Bases and PNA Base Monomers to Gold Nanoparticles. *J. Am. Chem. Soc.* **2004,** *126*, 13186-13187.

(47) Storhoff, J. J.; Elghanian, R.; Mucic, R. C.; Mirkin, C. A.; Letsinger, R. L. One-Pot Colorimetric Differentiation of Polynucleotides with Single Base Imperfections Using Gold Nanoparticle Probes. *J. Am. Chem. Soc.* **1998,** *120*, 1959-1964.

(48) Zhang, X.; Servos, M. R.; Liu, J. Ultrahigh Nanoparticle Stability against Salt, pH and Solvent with Retained Surface Accessibility via Depletion Stabilization. *J. Am. Chem. Soc.* **2012,** *134*, 9910-9913.